Nat. Hazards Earth Syst. Sci., 22, 2543–2551, 2022
https://doi.org/10.5194/nhess-22-2543-2022

Natural Hazards and Earth System Sciences
Open Access
EGU

Analysis of seismic strain release related to the tidal stress preceding the 2008 Wenchuan earthquake

Xuezhong Chen[1], **Yane Li**[1], **and Lijuan Chen**[2]

[1]Institute of Geophysics, China Earthquake Administration, Beijing 100081, China
[2]Chongqing Earthquake Administration, Chongqing 401147, China

Correspondence: Yane Li (luckystarabcd@163.com) and Xuezhong Chen (cxz8675@163.com)

Received: 22 December 2021 – Discussion started: 26 January 2022
Revised: 28 May 2022 – Accepted: 25 July 2022 – Published: 9 August 2022

Abstract. Tidal stresses could load or unload focal media and trigger small to moderate earthquakes in and around the focal region before a large or great earthquake. Based on the preliminary reference Earth model, we calculated the time series of tidal Coulomb failure stress (TCFS) acting on the focal fault plane of the Wenchuan earthquake. For earthquakes ($2.5 \leq M_L \leq 4.0$) that occurred in and around the focal region from January 1990 to April 2008, we calculated the time rate of TCFS, ΔTCFS, at the occurrence time of each earthquake. These earthquakes were divided into two categories on the basis of the signs of ΔTCFS: one is positive earthquakes (PEQs) occurring at times of $\Delta\text{TCFS} > 0$ and the other negative earthquakes (NEQs) occurring at times of $\Delta\text{TCFS} < 0$.

First, we obtained cumulative seismic strain release (CSSR) curves of NEQs and PEQs and found that the two curves nearly overlapped prior to September 2004 and then began to separate increasingly with time. We used a parameter R_p, the proportion of seismic strain release of PEQs, to investigate the effect of TCFS on earthquake occurrence and found that R_p was significantly higher than 0.5 about 6 months before the Wenchuan event at a 99 % confidence level, indicating a significant correlation between earthquake occurrence and increasing TCFS.

Furthermore, we calculated the slope k (time rate) of the CSSR curve vs. time for PEQs and NEQs separately. It was observed in the pre-event period that the seismic strain release accelerated when TCFS increased but decelerated when TCFS decreased. The difference in the time rate of seismic strain release between PEQs and NEQs was quantified using R_k, the ratio of k for PEQs to that for NEQs. We discovered stable R_k values (around 1.0) until they began to rise rapidly with time in early 2005, reaching their highest value of 2.7 just before the Wenchuan event. R_k could reveal the promoting and inhibiting effects of tidal stress on seismic strain release. When k_p increases alone or k_n decreases alone, R_k will increase. Thus, an increase in R_k corresponds to a promoting effect during times of increasing TCFS and an inhibiting one during that of decreasing TCFS. Both effects were observed in the focal region prior to the Wenchuan mainshock.

The b value in the Gutenberg–Richter relationship decreases as the tectonic stress in the crust increases. We also calculated the temporal evolution of the b value in the study region. It was observed that after 2.5 years of increasing tectonic stress, the focal region became unstable, and the tidal stress began to take effect. The effects of the tidal stress were gradually enhanced as the tectonic stress increased further. The increase in the tidal Coulomb failure stress may have aided the occurrence of earthquakes, whereas the decrease had the opposite effect. This observation may shed light on the seismogenic processes that led to the Wenchuan earthquake and its precursors.

1 Introduction

An M_s 8.0 earthquake occurred in Wenchuan County, province of Sichuan, China, on 12 May 2008, with an epicenter at 31.0° N, 103.4° E and a depth of 19 km, rupturing along the Longmenshan fault (indicated by F in Fig. 1a). It killed thousands of people, caused damage to buildings, triggered widespread landslides, and was followed by floods and epidemic outbreaks (Yan et al., 2009; Cao et al., 2010; Zhu

and Wang, 2013), along with serious impact on the ecological environment (Huang et al., 2018).

Scientists have reported their research on the Wenchuan earthquake, including the co-seismic changes in water level and water temperature associated with the Wenchuan earthquake (He et al., 2016, 2017; He and Singh, 2019), the changes in the b value (Zhao and Wu, 2008; Shi et al., 2018; Chen and Zhu, 2020), the tide-triggered earthquakes (Li and Chen, 2018), and correlation between the earthquake occurrence and Earth's rotation in the pre-mainshock (Chen and Li, 2019). Meanwhile, this paper focuses on the seismic strain release associated with the tidal stress prior to the 2008 Wenchuan earthquake.

The amplitude of stresses caused by the solid Earth tides in the crust is ~ 1 kPa, much lower than the average earthquake stress drop ($\sim 10^3$–10^4 kPa), and these stresses cannot provide the energy released in earthquakes. However, if the tectonic stress in the focal region reaches a critical value, the tidal stress could trigger an earthquake (Rydelek et al., 1992). Numerous studies have examined correlations between Earth tides and earthquakes. Positive correlation for aftershocks, volcanic earthquakes and small to large earthquakes have been obtained (Ryall, 1968; Shlien, 1972; Kayano, 1973; Filson et al., 1973; Mauk and Kienle, 1973; Tamrazyan, 1974; Klein, 1976; Gao et al., 1981; Kilston and Knopoff, 1983; Rydelek et al., 1988; Wilcock, 2001; Stroup et al., 2007; Zhang et al., 2007; Li and Jiang, 2011; Vergos et al., 2015), but there have been some exceptions (Schuster, 1897; Knopoff, 1964; Shlien, 1972; Heaton, 1982; Rydelek et al., 1992; Tanaka et al., 2006). It seems that tidal triggering of earthquakes with dip-slip or oblique-slip focal mechanisms may be more significant (Heaton, 1975; Tsuruoka et al., 1995; Tanaka et al., 2002a; Cochran et al., 2004; Li and Zhang, 2011; Bucholc and Steacy, 2016). Tidal stress triggered shallow strike-slip earthquakes that occurred in or near mainland China, but oblique-slip or dip-slip earthquakes in the same area were not triggered by tidal stresses and nor were strike-slip earthquakes occurring in California, USA (Ding et al., 1983; Vidale et al., 1998). No statistically significant evidence for a focal mechanism dependence on earthquake tidal triggering was found in the National Earthquake Information Center (NEIC) catalog (Métivier et al., 2009). The effect of tidal Coulomb stress triggering is more significant for normal slip earthquakes at low and middle latitudes and reverse-slip earthquakes at middle and high latitudes, and the tidal stress triggering decreases with increasing latitude for strike-slip earthquakes (Xu et al., 2011). A high correlation between Earth tides and earthquake occurrence was detected in and around the epicenters in the several years prior to some moderate to large earthquakes (Chen and Ding, 1996; Chen et al., 1998; Tanaka et al., 2002b; Tanaka, 2010, 2012; Li and Chen, 2018).

Researchers have shown interest in the seismic strain (or moment) release acceleration near the epicentral area before strong earthquakes. Accelerating seismic strain release has been reported before some earthquakes; however, before other cases the seismic strain release does not significantly accelerate and even decelerates (Sykes and Jaumé, 1990; Bufe and Varnes, 1993; Brehm and Braile, 1998, 1999; Bowman et al., 1998; Yang and Ma, 1999; Jiang et al., 2004; C. S. Jiang et al., 2009; H. K. Jiang et al., 2009a, b; Zhang et al., 2014; Li et al., 2015; Qian et al., 2015). Typically, researchers have investigated the accelerating seismic strain release before strong earthquakes using the method proposed by Bufe and Varnes (1993), which is based on the cumulative seismic strain release curve of small to moderate earthquakes occurring near the epicenter over a specific time period (often several years to tens of years) before the strong earthquakes. They presented their findings to demonstrate whether there is a significant accelerating seismic strain release. They analyzed the shape of the seismic strain release curve as a function of time by considering the studied period as a whole. The curve of seismic strain release over a longer time can be viewed as a chain of straight lines with various slopes. When the seismic strain release accelerates, the slope of the straight lines will become greater and greater and vice versa.

We will examine whether there was any difference in the seismic strain release when the tidal stress increased and when it decreased for earthquakes that occurred before the 2008 M_s 8.0 Wenchuan earthquake based on the above idea and consider the effects of the tidal stress.

2 Study region and data used

Earthquakes used in this study were obtained from the China Earthquake Networks Center, China Earthquake Administration. The Wenchuan earthquake's aftershocks ($M_L \geq 3.0$) that occurred from 12 May to 31 August 2008 are plotted in Fig. 1a. The aftershocks extended ~ 350 km to the northeast. A very large part of fault slip during the occurrence of the Wenchuan mainshock took place within a region between Maoxian and the town of Dachuan in the southwestern aftershock zone (Zhang et al., 2008); meanwhile larger values of seismic strain release for aftershocks from 12 to 31 May 2008 were located within the same region. This region, enclosed by a quadrangle with a length of ~ 140 km in Fig. 1b, was defined as the study region in this article due to its significant correlation with the occurrence of the Wenchuan mainshock.

The magnitudes versus time for earthquakes ($M_L \geq 2.0$) that occurred in the study region between January 1990 and April 2008 is plotted in Fig. 2a. It can be seen that fewer earthquakes with $M_L \geq 2.0$ occurred before 2000, resulting from the sparse seismic stations situated in and around the study region. The observed Gutenberg–Richter (G–R) relationship is usually used for determination of the threshold of completeness of the earthquake catalogue via inspection. The G–R relationships are plotted in Fig. 2b for earthquakes before and after 2000. The plot suggests the threshold of completeness to be $M_c = 2.5$ before 2000 and $M_c = 1.5$ af-

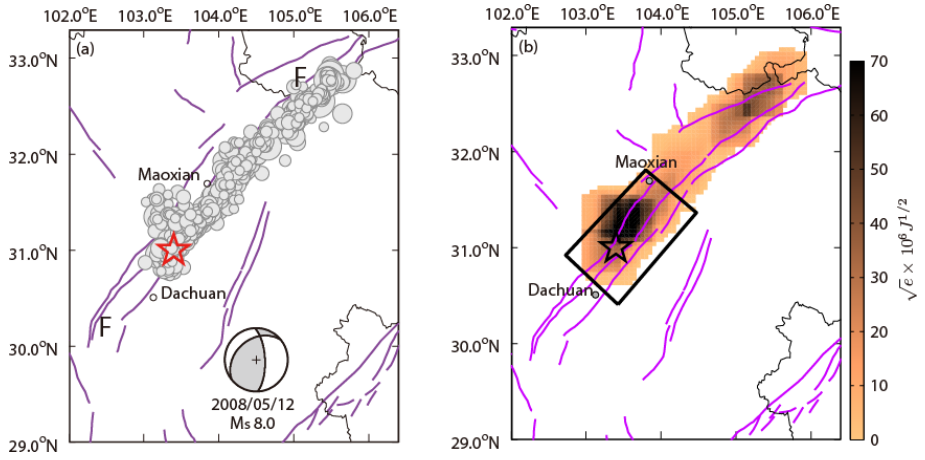

Figure 1. **(a)** Map showing the locations of aftershocks ($M_L \geq 3.0$) following the Wenchuan event from 12 May to 31 August 2008. The focal mechanism solution comes from the Global Centroid Moment Tensor (CMT) catalog. "F" represents the Longmenshan fault. **(b)** The spatial distribution of seismic strain for the aftershocks that occurred from 12 to 31 May 2008. The star shows the epicenter of the Wenchuan event. The quadrangle shows the study region.

ter that. It can also be found from the G–R relationship that earthquakes with a magnitude $M_L > 4.0$ do not obey the linear relationship. After we exclude those $M_L > 4.0$ earthquakes, 217 earthquakes with a magnitude span of $2.5 \leq M_L \leq 4.0$ are used in this study.

3 Analytical method

Based on the preliminary reference Earth model (Dziewonski and Anderson, 1981), the tide-generating stress components in the Earth's interior are calculated. The potential due to the attraction of the Moon and the Sun at point A (r, θ, λ) can be written as follows (Luo et al., 1986):

$$\left.\begin{aligned} V_m(A) &= \tfrac{3}{4} D \frac{C_m^3}{r_m} \frac{1}{R^2} \sum_{n=2}^{\infty} \left(\frac{r}{r_m}\right)^n P_n(\cos Z_m) \\ V_s(A) &= \tfrac{3}{4} D_s \frac{C_s^3}{r_s} \frac{1}{R^2} \sum_{n=2}^{\infty} \left(\frac{r}{r_s}\right)^n P_n(\cos Z_s) \end{aligned}\right\}, \quad (1)$$

where D is 26 277 cm^2 s^{-2}; the Doodson constant is $D_s = 0.45924$ D; r_m is the distance between the center of the Earth and the Moon; r_s is the distance between the center of the Earth and the Sun; r is the radius from the Earth's center; Z_m is the geocentric zenith distance of the Moon at point A; Z_s is the geocentric zenith distance of the Sun at point A; R is the Earth's mean radius (taken to be 6 371 024 m); C_m is the average distance between the Earth and the Moon, equal to 3.844×10^8 m; C_s is the average distance between the Earth and the Sun, equal to 1.496×10^{11} m; λ is easterly longitude; and θ is colatitude.

The radial, colatitudinal and longitudinal displacements caused by the potential are given by

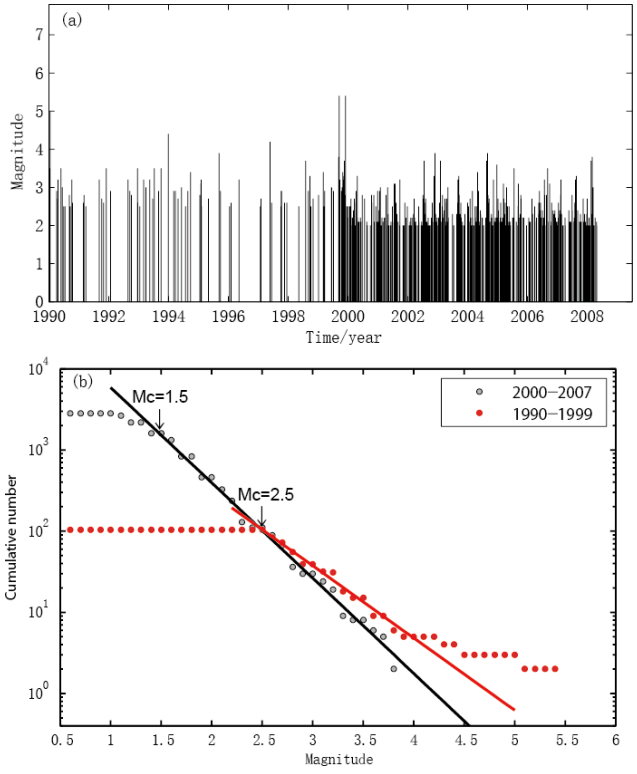

Figure 2. **(a)** Magnitude as a function of time for earthquakes ($M_L \geq 2.0$) occurring in the study region. **(b)** Cumulative number vs. magnitude for earthquakes in the study region.

$$\left.\begin{aligned} u_{\mathrm{r}}(A) &= \sum_{n=2}^{\infty} \frac{H_{\mathrm{n}}(r)}{g(r)} V_{\mathrm{n}}(A) \\ u_{\theta}(A) &= \sum_{n=2}^{\infty} \frac{L_{\mathrm{n}}(r)}{g(r)} \frac{\partial V_{\mathrm{n}}(A)}{\partial \theta} \\ u_{\lambda}(A) &= \sum_{n=2}^{\infty} \frac{L_{\mathrm{n}}(r)}{g(r)} \frac{\partial V_{\mathrm{n}}(A)}{\partial \lambda} \end{aligned}\right\}, \tag{2}$$

where $V_{\mathrm{n}} = V_{\mathrm{m}} + V_{\mathrm{s}}$, $g(r)$ is the acceleration due to gravity. $H_{\mathrm{n}}(r)$ and $L_{\mathrm{n}}(r)$ are Love's numbers.

The strain components are obtained by

$$\left.\begin{aligned} \varepsilon_{\mathrm{r}} &= \frac{\partial u_{\mathrm{r}}}{\partial r} \\ \varepsilon_{\theta} &= \frac{u_{\mathrm{r}}}{r} + \frac{\partial u_{\theta}}{r \partial \theta} \\ \varepsilon_{\lambda} &= \frac{u_{\mathrm{r}} + u_{\theta} \cot\theta}{r} + \frac{\partial u_{\lambda}}{r \sin\theta \partial \lambda} \\ \varepsilon_{\mathrm{r}\theta} &= \frac{\partial u_{\mathrm{r}}}{r \partial \theta} + \frac{\partial u_{\theta}}{\partial r} - \frac{u_{\theta}}{r} \\ \varepsilon_{\mathrm{r}\lambda} &= \frac{1}{r \sin\theta} \frac{\partial u_{\lambda}}{\partial \lambda} + \frac{\partial u_{\lambda}}{\partial r} - \frac{u_{\lambda}}{r} \\ \varepsilon_{\lambda\theta} &= \frac{1}{r} \left(\frac{\partial u_{\lambda}}{\partial \theta} - u_{\lambda} \cot\theta \right) + \frac{1}{r \sin\theta} \frac{\partial u_{\theta}}{\partial \lambda} \end{aligned}\right\}. \tag{3}$$

The stress components are obtained by

$$\tau_{ij} = \lambda' \Theta \delta_{ij} + 2\mu \varepsilon_{ij} \ , \tag{4}$$

where λ' and μ are Lamé's coefficients, Θ is bulk strain, and δ_{ij} is the Kronecker operator.

According to the focal mechanism solution of the Wenchuan earthquake, the tidal stress components are projected onto its focal fault plane. The tidal normal stress σ_{n} and shear stress τ can be obtained, and then the tidal Coulomb failure stress (TCFS) acting on the focal fault plane can be obtained by applying Eq. (5):

$$\mathrm{TCFS} = \tau + \mu \sigma_{\mathrm{n}} \ , \tag{5}$$

where μ is the coefficient of friction, taken to be 0.6 (Chen, 1988). According to the Global CMT catalog, the focal fault plane of the Wenchuan earthquake is a thrust-type one with the geometry of strike being 231° and dip being 35°. The rake is 138°. In calculation, the focal depth was taken to be 19 km. Figure 3 shows the temporal variations in TCFS caused by tides on the focal fault plane of the Wenchuan earthquake at a depth of 19 km.

We calculated the time series of TCFS at the epicenter of each earthquake. Based on the time series, we also calculated the TCFS rate (ΔTCFS) at the occurrence time of each earthquake. When TCFS increases, $\Delta\mathrm{TCFS} > 0$ and vice versa. Earthquakes were divided into two categories: positive earthquakes (PEQs) occurring at times of $\Delta\mathrm{TCFS} > 0$ and negative earthquakes (NEQs) occurring at times of $\Delta\mathrm{TCFS} < 0$. Thus, the characteristics of the seismic strain released during positive and negative TCFS can be analyzed using the above information.

In seismology, the seismic strain release ε is represented by the Benioff strain obtained by taking the square root of seismic energy E_{s} calculated from Eq. (6) (Gutenberg and Richter, 1956). For earthquakes in mainland China, M_{s} in Eq. (6) can be obtained from M_{L} by Eq. (7) (Fu and Liu, 1991). We arranged the earthquakes in chronological order and then obtained the cumulative seismic strain release (CSSR) versus time by accumulating their Benioff strain values.

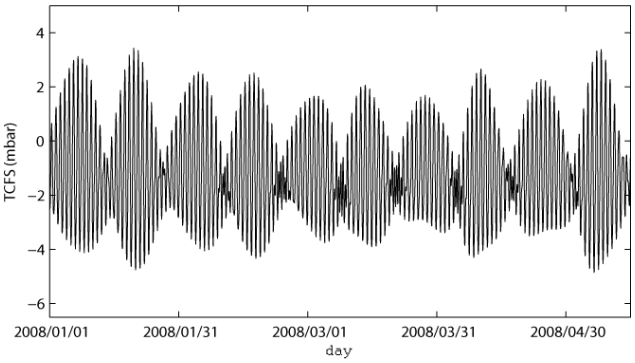

Figure 3. Temporal variations in TCFS caused on the focal fault plane of the Wenchuan earthquake at a depth of 19 km. The date is given in the format year/month/day.

$$\log E_{\mathrm{s}} = 1.5 M_{\mathrm{s}} + 4.8 \tag{6}$$

$$M_{\mathrm{s}} = 1.13 M_{\mathrm{L}} - 1.08 \tag{7}$$

4 Results

Figure 4a shows the CSSR curves of NEQs and PEQs. The CSSR curve for PEQs is represented by grey circles, while cyan squares represent the CSSR curve for NEQs. The two curves almost overlapped before September 2004. However, they began to diverge increasingly with time, indicating that the seismic strain release of PEQs was higher than that of NEQs.

The proportion of seismic strain release for PEQs R_{p} as a function of time was calculated using a 3-monthly moving 5-year time window. R_{p} is defined as

$$R_{\mathrm{p}} = \frac{\varepsilon_{\mathrm{p}}}{n}, \tag{8}$$

where ε is the total seismic strain release of PEQs and NEQs and ε_{p} is that of PEQs. Figure 4b depicts R_{p} vs. time. It ranged between 0.3 and 0.6 prior to October 2007; then it surpassed 0.7. As the length of time with $\Delta\mathrm{TCFS} > 0$ is approximately equal to that with $\Delta\mathrm{TCFS} < 0$, if the tidal Coulomb failure stress does not affect earthquakes, the normal value of R_{p} is 0.5, and if increasing TCFS affects seismic strain release, R_{p} should be significantly greater than 0.5, as measured by its z values (Ge and Wang, 2006). The z value of N earthquakes can be calculated according to Eq. (9):

$$z = \left(2R_{\mathrm{p}} - 1\right)\sqrt{N}, \tag{9}$$

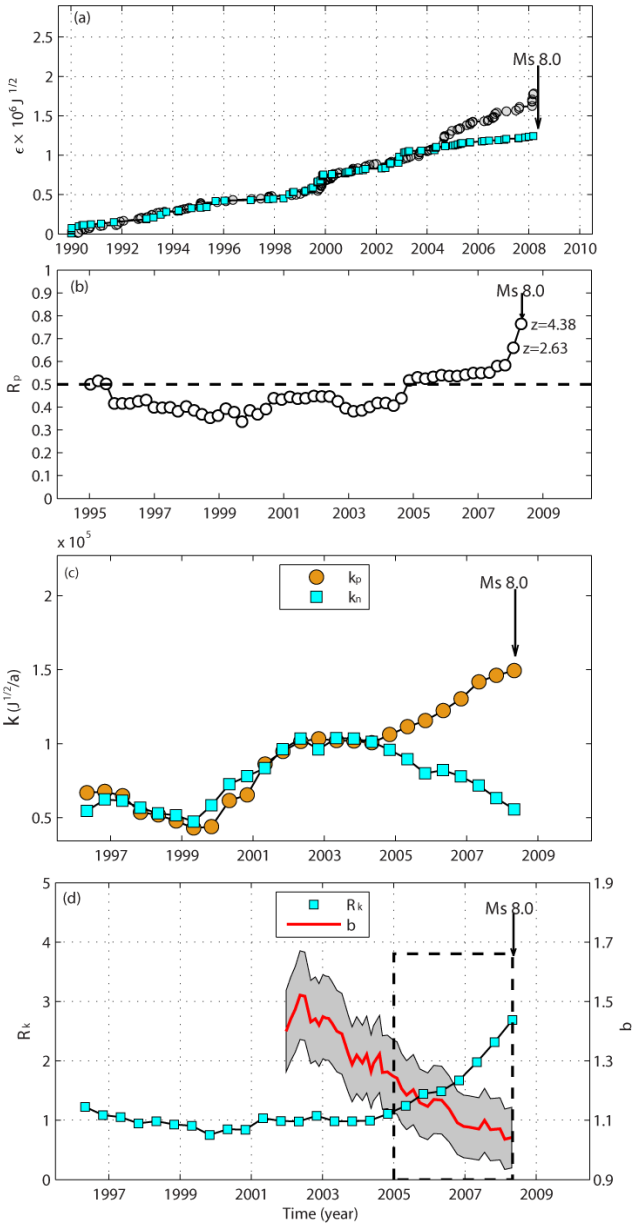

Figure 4. **(a)** Cumulative seismic strain release curve. The line with ◯ symbols is for PEQs, and the line with □ symbols is for NEQs. **(b)** R_p vs. time, with a moving 6-year time window moved by 6 months. **(c)** The time rate k of CSSR vs. time for both PEQs and NEQs. The orange circles show the time rate k for PEQs, and the cyan squares are for NEQs, with a moving 6-year time window moved by 6 months. **(d)** R_k (cyan squares) and b value (red line) as a function of time. The grey area indicates the 95 % confidence limit of the b value. The downward arrow shows the occurrence of the Wenchuan earthquake.

Table 1. The values of z_α at different significance levels.

α	z_α	α	z_α
0.001	3.29	0.01	2.575
0.002	3.09	0.02	2.336
0.005	2.81	0.05	1.96

where N is the total number of earthquakes used to calculate R_p. The critical z value is denoted by z_α, for which values at different significance levels are shown in Table 1. The z values for the last two R_p values in Fig. 4b are 2.63 and 4.38, indicating a significant difference between the two R_p values and 0.5 at a 99 % confidence level. Thus, the seismic strain release was significantly related to the increasing tidal Coulomb failure stress.

The slope, k, of the CSSR curve can represent the time rate of seismic strain release. The seismic strain release accelerates as the slope increases and vice versa. The observed slope as a function of time was obtained by fitting the data with straight lines over a 6-year time window that moved in 6-month steps. Let k_p denote the slope for PEQs and k_n that for NEQs; both are shown in Fig. 4c using the orange circles "◯" for k_p and the cyan squares "□" for k_n. The seismic strain release accelerates for PEQs when k_p increases and for NEQs when k_n increases. k_p and k_n had almost the same value simultaneously and were in phase before 2005. After that, they changed to out of phase, and k_p increased with time, whereas k_n decreased. Thus, even in the several years before the Wenchuan event, the seismic strain release accelerated when the tidal Coulomb failure stress increased. At the same time, it decelerated when the tidal Coulomb failure stress decreased.

We analyzed the difference between k_p and k_n using their ratio R_k defined as

$$R_k = \frac{k_p}{k_n}. \tag{10}$$

It can be seen from R_k vs. time, as shown in Fig. 4d, that R_k began to rise rapidly in early 2005, reaching its peak value just before the Wenchuan earthquake. This means that, compared to NEQs, the seismic strain release rate for PEQs increased dramatically before the Wenchuan earthquake. Just before the Wenchuan event, k_p reached ~ 2.7-fold more than k_n.

The decrease in parameter b in the G–R relationship $\log N(M) = a - bM$ is interpreted as a stress increase in the crust before an upcoming seismic event (Scholz, 1968; Wyss, 1973). We investigated the temporal changes in crustal stress by the b value in the study region to analyze the relationship between R_k and the regional tectonic stress. The maximum likelihood method was used to calculate the b value (Aki, 1965):

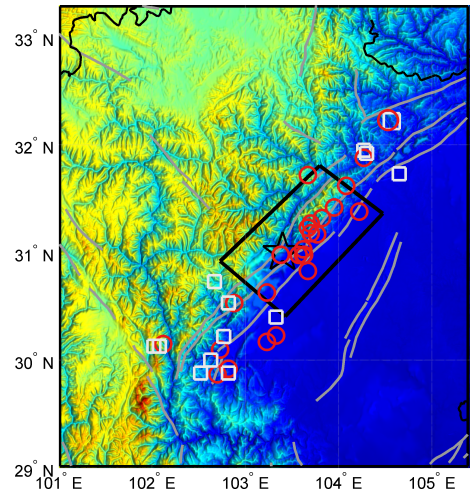

Figure 5. Epicentral distribution of PEQs (red circles) and NEQs (white squares) ($M_L \geq 3.0$) that occurred along the Longmenshan fault from January 2005 to April 2008. The star shows the epicenter of the Wenchuan event.

$$b = \frac{\log e}{\overline{M} - M_{\min}}. \tag{11}$$

The 95 % confidence standard deviation of b is

$$\sigma(b) = 1.96\frac{b}{\sqrt{N-1}}, \tag{12}$$

where $\overline{M}$ represents the average magnitude of a group of earthquakes and $M_{\min}$ is the minimum magnitude in the group. We calculated the b value as a function of time using the earthquakes with $M_L \geq 1.5$ in the study region from January 2000 to April 2008 because fewer earthquakes occurred before 2000. Calculations of $b(t)$ were performed in sliding time windows with a constant number of 400 events that advanced in steps of 30 events. The red line shows the temporal changes in the b value in Fig. 4d, and the grey area indicates the 95 % confidence interval. In the 6 years leading up to the Wenchuan event, the b value dropped by 31.6 %, from 1.52 in May 2002 to 1.04 just before the event. Before 2005, it decreased by 17.8 % and 13.8 % in the last 3 years and 4 months respectively. Stable R_k values (around 1.0) are found during the previous period of decreasing b values, but when the b value dropped to 1.25 at the end of 2004, R_k started to rise, and the b value continued to fall while R_k increased rapidly, eventually reaching 2.7.

The b value can reflect the regional tectonic stress, with a decrease in its value corresponding to an increase in regional tectonic stress. Therefore, R_k remained stable, around 1, during the early stage of the regional tectonic stress enhancement, indicating that TCFS did not affect seismic strain release, but R_k was rapidly enhanced as the regional tectonic stress increased, reaching a maximum value of 2.7 as the Wenchuan mainshock approached (see the dashed black frame in Fig. 4d). This means that the rate at which the seismic strain was released during the time of increasing TCFS was $\sim$ 2.7-fold greater than that during the time of decreasing TCFS when the focal source region of the Wenchuan event was approaching instability.

To summarize the preceding observations, there was a significant stress buildup around the epicentral area preceding the Wenchuan mainshock. The difference in seismic strain release between earthquakes that occurred when TCFS increased and those occurring when TCFS decreased became increasingly noticeable during the latter phase of the stress buildup and peaked just before the Wenchuan mainshock.

5 Conclusions and discussions

In the present article, we examined the difference in seismic strain release between earthquakes that occurred during the increase in tidal Coulomb failure stress and those that happened during the decrease preceding the Wenchuan earthquake. The obtained results are as follows:

1. The proportion of seismic strain released during the increase period of the tidal Coulomb failure stress was significantly greater than 0.5 at the 99 % confidence level around the epicentral area about 6 months before the Wenchuan event, indicating a significant correlation between the earthquake occurrence and increasing tidal Coulomb failure stress.

2. For several years prior to the Wenchuan event, the seismic strain release accelerated during periods of increasing tidal Coulomb failure stress and decelerated during decreasing tidal Coulomb failure stress.

3. When the Wenchuan earthquake was approaching, the ratio (R_k) of the time rate of seismic strain release during the increased time interval of tidal Coulomb failure stress to that during the decreased time interval increased rapidly, reaching $\sim$ 2.7.

The b value, which is related to the tectonic stress in the crust, had been declining since May 2002, until the Wenchuan event. By comparing ratio R_k with the b value, it can be found that the tidal Coulomb failure stress did not affect the seismic strain release in the early period of tectonic stress buildup. However, as tectonic stress increased further, the difference in seismic strain release between NEQs and PEQs became apparent. The difference grew gradually over time, and the effect of tidal Coulomb failure stress on seismic strain release became increasingly significant.

The Earth tides produce cyclic stress variations in the Earth. These stress variations, which are of the order of 10^3–10^4 Pa, are small in comparison to tectonic stresses. When the tectonic stress in a focal region is low, tidal stress does

not affect earthquakes. However, when it is close to a critical condition for releasing a large rupture, the tidal stress may affect the earthquake occurrence. The increase in tidal stress promotes the earthquake occurrence, causing strain release acceleration for PEQs (corresponding to the rise in k_p in Fig. 4c). In contrast, the decrease in tidal stress inhibits the earthquake occurrence, causing strain release deceleration for NEQs (corresponding to the decrease in k_n in Fig. 4c).

Figure 5 shows the epicentral distribution of PEQs and NEQs ($M_L \geq 3.0$) that occurred along the Longmenshan fault from January 2005 to April 2008. It can be seen from this figure that only PEQs (red circles) occurred in the study region and no $M_L \geq 3.0$ NEQs occurred there. Magnitudes as a function of time indicate that $M_L \geq 3.0$ PEQs occurred more frequently after 2005 than before. That might be the reason that k_n decreased and k_p increased. It must be pointed out that k_p and k_n both fluctuate due to the seismicity rate or other reasons. When the tidal stress does not take effect, they change synchronously without much difference between them; but when the tidal stress begins to take effect, they separate. So the separation is most important.

It can be concluded that the increase in tidal Coulomb failure stress in the 3 years or more before the Wenchuan earthquake might have aided the occurrence of earthquakes, whereas its decrease had the opposite effect. This observation could shed light on the processes that led to the Wenchuan earthquake and its precursors.

Code availability. The MATLAB code used in this research can be obtained from the corresponding authors.

Data availability. The earthquake catalog supporting the findings of this study is available in the China Earthquake Networks Center, China Earthquake Administration, and can be obtained by contacting the corresponding authors.

Supplement. The supplement related to this article is available online at: https://doi.org/10.5194/nhess-22-2543-2022-supplement.

Author contributions. XC contributed to the conceptualization; supervised the research; formulated the research questions; and specified the manuscript contents, discussed with YL and JC, and prepared the manuscript. YL participated in the collection of references, performed the collation of the earthquake catalog used and plotting diagrams, submitted the manuscript, and provided constructive suggestions to the study. JC participated in the collection of references and provided constructive suggestions to the study.

Competing interests. The contact author has declared that none of the authors has any competing interests.

Disclaimer. Publisher's note: Copernicus Publications remains neutral with regard to jurisdictional claims in published maps and institutional affiliations.

Acknowledgements. The authors sincerely express their thanks to the journal editors for their help and comments beneficial to the manuscript.

Financial support. This research has been supported by the National Key Research and Development Program of China, Chinese Polar Environment Comprehensive Investigation and Assessment Programmes (grant no. 2018YFC1503400).

Review statement. This paper was edited by Oded Katz and reviewed by Andrew Delorey and one anonymous referee.

References

Aki, K.: Maximum likelihood estimate of b in the formula $\log N = a - bM$ and its confidence limits, Bull. Earthq. Res. Inst. Univ. Tokyo, 43, 237–239, 1965.

Bowman, D. D., Ouillon, G., Sammis, C. G., Sornette, A., and Sornette, D.: An observational test of the critical earthquake concept, J. Geophys. Res., 103, 24359–24372, 1998.

Brehm, D. J. and Braile, L. W.: Application of the time-to-failure method for intermediate-term prediction in the New Madrid seismic zone, Bull. Seismol. Soc. Am., 88, 564–580, 1998.

Brehm, D. J. and Braile, L. W.: Intermediate-term earthquake prediction using the modified time-to-failure method in southern California, Bull. Seismol. Soc. Am., 89, 275–293, 1999.

Bucholc, M. and Steacy, S.: Tidal stress triggering of earthquakes in Southern California, Geophys. J. Int., 205, 681–693, https://doi.org/10.1093/gji/ggw045, 2016.

Bufe, C. G. and Varnes, D. J.: Predictive modeling of the seismic cycle of the great San Francisco Bay region, J. Geophys. Res., 98, 9871–9883, 1993.

Cao, C. X., Chang, C. Y., Xu, M., Zhao, J., Gao, M. X., Zhang, H., Guo, J. P., Guo, J. H., Dong, L., He, Q. S., Bai, L. Y., Bao, Y. F., Chen, W., Zheng, S., Tian, Y. F., Li, W. X., and Li, X. W.: Epidemic risk analysis after the Wenchuan earthquake using remote sensing, Int. J. Remote Sens., 31, 3631–3642, 2010.

Chen, J.and Zhu, S. B.: Spatial and temporal b-value precursors preceding the 2008 Wenchuan,China,earthquake(Mw=7.9): implications for earthquake prediction, Geomat. Nat. Hazards Risk, 11, 1196–1211, https://doi.org/10.1080/19475705.2020.1784297, 2020.

Chen, R. H. and Ding, X.: Distribution of local mean lunar times of significant shocks in source region and its vicinity before large earthquake and its explanation, Chinese J. Geophys., 39, 224–230, 1996.

Chen, X. and Li, Y.: Relationship Between the deceleration of Earth's rotation and earthquakes that occurred before the M_S 8.0 Wenchuan earthquake, Pure Appl. Geophys., 176, 5253–5260, https://doi.org/10.1007/s00024-019-02273-6, 2019.

Chen, X. Z., Zhong. N. C., and Ding, J. H.: The effect of lunar phase of seismicity in north China and its significance to earthquake prediction, Earthquake, 18, 325–330, 1998.

Chen, Y.: Mechanical properties of crustal rocks, Seismological Press, Beijing, China, 58 pp., ISNB 7-5028-0020-4/P.19, 1988.

Cochran, E. S., Vidale, J. E., and Tanaka, S.: Earth tides can trigger shallow thrust fault earthquakes, Science, 306, 1164–1166, https://doi.org/10.1126/science.1103961, 2004.

Ding, Z., Jia. J., and Wang, R.: Seismic triggering effect of tidal stress, Acta Seismol. Sinica, 5, 172-184, 1983(in Chinese with English abstract).

Dziewonski, A. M. and Anderson, D. L.: Preliminary reference earth model, Phys. Planet. Iner., 25, 297–356, 1981.

Filson, J., Simkin, T., and Leu, L.: Seismicity of a caldera collapse: Galapagos Islands 1968, J. Geophys. Res., 78, 8591, https://doi.org/10.1029/jb078i035p08591, 1973.

Fu, S. F. and Liu, B. C.: Courses of seismology, Seismological Press, Beijing, China, 476 pp., ISBN 7-5028-0426-9/G.13, 1991.

Gao, X. M., Yin, Z. S., Wang, W. Z., Huang, L. J., and Li, J.: Triggering of earthquakes by the tidal stress tensor, Acta Seismol. Sin., 3, 264–275, 1981.

Ge, X. Q. and Wang, B.: Applied statistics, Social Sciences Academic Press, Beijing, China, 75–76, ISBN 7-80230-132-7/F.019, 2006.

Gutenberg, B. and Richter, C. F.: Magnitude and energy of earthquakes, Annali di Geofisica, 9, 1–15, 1956.

He, A. and Singh, R. P.: Groundwater level response to the Wenchuan earthquake of May 2008, Geomat. Nat. Hazards Risk, 10, 336–352, 2019.

He, A., Singh, R. P., Sun, Z., Ye, Q., and Zhao, G.: Comparison of regression methods to compute atmospheric pressure and earth tidal coefficients in water level associated with Wenchuan Earthquake of 12 May 2008, Pure Appl. Geophys., 173, 2277–2294, https://doi.org/10.1007/s00024-016-1310-3, 2016.

He, A., Zhao, G., Sun, Z., and Singh, R. P.: Co-seismic multilayer water temperature and water level changes associated with Wenchuan and Tohoku-Oki earthquakes in the Chuan no. 3 well China, J. Seismol., 21, 719–734, https://doi.org/10.1007/s10950-016-9631-3, 2017.

Heaton, T. H.: Tidal triggering of earthquakes, Geophys. J. R. Astr. Soc., 43, 307–326, 1975.

Heaton, T. H.: Tidal triggering of earthquakes, Bull. Seismol. Soc. Am., 72, 2181–2200, 1982.

Huang, Z., Xu, M., Chen, W., Lin, X., Cao, C., and Singh, R. P.: Post-seismic Restoration of the Ecological Environment in the Wenchuan Region Using Satellite Data, Sustainability, 10, 3990, https://doi.org/10.3390/su10113990, 2018.

Jiang, C. S., Wu, Z. L., and Shi, Y. J.: Generality of accelerating moment release (AMR) before moderately strong earthquakes, Earthq. Res. China, 20, 119–125, 2004.

Jiang, C. S., Wu, Z. L., and Shi, Y. J.: Accelerating moment release (AMR) before strong earthquakes – A retrospective case study of a controversial precursor, Chinese J. Geophys., 52, 691–702, 2009.

Jiang, H. K., Wu, Q., Dong, X., Miao, Q. Z., and Song, J.: Behaviors of AE strain release under the different temperature and pressure condition: Discussion on the physical meanings of ASR model parameter, Chinese J. Geophys., 52, 2064–2073, 2009a.

Jiang, H. K., Miao, Q. Z., Dong, X., Wu, Q., Li, M. X., and Song, J., X.: Characteristics of strain release before *M* 7 earthquakes in mainland China, Earthquake, 29, 1–11, 2009b.

Kayano, I.: Microearthquake activity in Hiroshima and Shimane Prefectures and surrounding areas, Western Japan, Bull. Earthq. Res. Inst., 26, 178–203, https://doi.org/10.4294/zisin1948.26.2_178, 1973.

Kilston, S. and Knopoff, L.: Lunar-solar periodicitis of large earthquakes in southern California, Nature, 304, 21–25, 1983.

Klein, F. W.: Earthquake swarms and the semidiurnal solid earth tide, Geophys. J. R. Astr. Soc., 45, 245–295, 1976.

Knopoff, J.: Earth tides as a triggering mechanism for earthquakes, Bull. Seismol. Soc. Am., 54, 1865–1870, 1964.

Li, J. and Jiang, H. K.: A statistical analysis on Wenchuan aftershock activity triggered by earth tide, Earthq. Res. China, 27, 363–375, 2011.

Li, X., Jiang, C. S., Yan, D. Q., Zhang, Z. H., Yin, X. H., Chen, C. H., and Wan, Z.: Research on spatial scanning characteristic of accelerating moment release before moderate-strong earthquakes in north China region since 1989, J. Seismol. Res., 38, 359–369, 2015.

Li, Y. and Chen, X.: Earth tidal stress as an earthquake trigger prior to the Wenchuan earthquake, Sichuan, China, Chin. Sci. Bull., 63, 1962–1970, https://doi.org/10.1360/N972018-00259, 2018.

Li, Z. and Zhang, X.: Relationship of tidal stress and large earthquakes, Earthquake, 31, 48–57, 2011.

Luo, M. J., Gu, M. L., Sui, J. S., and Li, A. Y.: Calculation of the theoretical values of the strain tide, Chinese J. Geophys., 29, 157–165, 1986.

Mauk, F. J. and Kienle, J.: Microearthquakes at St. Augustine volcano, Alaska, triggered by earth tides, Science, 182, 386–389, https://doi.org/10.1126/science.182.4110.386, 1973.

Métivier, L., de Viron, O., Conrad, C. P., Renault, S., Diament, M., and Patau, G.: Evidence of earthquake triggering by the solid earth tides, Earth Planet. Sc. Lett., 278, 370–375, https://doi.org/10.1016/j.epsl.2008.12.024, 2009.

Qian, X. D., Li, Q., and Hong, M.: Characteristics of strain release before moderate-strong earthquakes in Yunnan region, Acta Seismol. Sin., 37, 386–401, 2015.

Ryall, A., Vanwormer, J. D., and Jones, A. E.: Triggering of microearthquakes by earth tides, and other features of the Truckee, California, earthquake sequence of September 1966, Bull. Seismol. Soc. Am., 58, 215–248, 1968.

Rydelek, P. A., Davis, P. M., and Koyanagi, R. Y.: Tidal triggering of earthquake swarms at Kilauea vocano, Hawaii, J. Geophys. Res., 93, 4401–4411, 1988.

Rydelek, P. A., Sacks, I. S., and Scarpa, R.: On tidal triggering of earthquakes at CampiFlegrei, Italy, Geophys. J. Int., 109, 125–137, https://doi.org/10.1111/j.1365-246X.1992.tb00083.x, 1992.

Scholz, C. H.: The frequency–magnitude relation of microfracturing in rock and its relation to earthquakes, Bull. Seismol. Soc. Am., 58, 399–415, 1968.

Schuster, A.: On lunar and solar periodicities of earthquakes, P. Roy. Soc. Lond., 61, 455–465, https://doi.org/10.1038/056321a0, 1897.

Shi, H. X., Meng, L. Y., Zhang, X. M., Chang, Y., Yang, Z. T., Xie, W. Y., Fu, B. K. Z., and Han, P.: Decrease in b value prior to the Wenchuan earthquake (M_S 8.0), Chinese J. Geophys., 61, 1874–1882, 2018.

Shlien, S.: Earthquake–tide correlation, Geophys. J. R. Astr. Soc., 28, 27–34, 1972.

Stroup, D. F., Bohnenstieh, D. R., Tolstoy, M., Waldhauser, F., and Weekly, R. T.: Pulse of the seafloor: Tidal triggering of microearthquakes at 9°50′ N East Pacific Rise, Geophys. Res. Lett., 34, L15301, https://doi.org/10.1029/2007GL030088, 2007.

Sykes, L. R. and Jaumé, S. C.: Seismic activity on neighbouring faults as a long-term precursor to large earthquakes in the San Francisco Bay area, Nature, 348, 595–599, 1990.

Tamrazyan, G. P.: Possible cosmic influences on the 1966 Tashkent earthquake and its largest aftershocks, Geophys. J. R. Astr. Soc., 38, 423–429, 1974.

Tanaka, S.: Tidal triggering of earthquakes precursory to the recent Sumatra megathrust earthquakes of 26 December 2004 (M_w 9.0), 28 March 2005 (M_w 8.6), and 12 September 2007 (M_w 8.5), Geophys. Res. Lett., 37, L02301, https://doi.org/10.1029/2009gl041581, 2010.

Tanaka, S.: Tidal triggering of earthquakes prior to the 2011 Tohoku-Oki earthquake (M_w 9.1), Geophys. Res. Lett., 39, L00G26, https://doi.org/10.1029/2012GL051179, 2012.

Tanaka, S., Ohtake, M., and Sato, H.: Evidence for tidal triggering of earthquakes as revealed from statistical analysis of global data, J. Geophys. Res., 107, 2211, https://doi.org/10.1029/2001JB001577, 2002a.

Tanaka, S., Ohtake, M., and Sato, H.: Spatio-temporal variation of the tidal triggering effect on earthquake occurrence associated with the 1982 South Tonga earthquake of M_w 7.5, Geophys. Res. Lett., 29, 3-1–3-4, https://doi.org/10.1029/2002GL015386, 2002b.

Tanaka, S., Sato, H., Matsumura, S., and Ohtake, M.: Tidal triggering of earthquakes in the subducting Philippine Sea plate beneath the locked zone of the plate interface in the Tokai region, Japan, Tectonophysics, 417, 69–80, https://doi.org/10.1016/j.tecto.2005.09.013, 2006.

Tsuruoka, H., Ohtake, M., and Sato, H.: Statistical test of the tidal triggering of earthquakes: Contribution of the ocean tide loading effect, Geophys. J. Int., 122, 183–194, https://doi.org/10.1111/j.1365-246X.1995.tb03546.x, 1995.

Vergos, G., Arabelos, D. N., and Contadakis, M. E.: Evidence for tidal triggering on the earthquakes of the Hellenic Arc, Greece, Phys. Chem. Earth Pt. A/B/C, 85–86, 210–215, https://doi.org/10.1016/j.pce.2015.02.004, 2015.

Vidale, J. E., Agnew, D. C., Johnston, M. J. S., and Oppenheimer, D. H.: Absence of earthquake correlation with Earth tides: an indication of high preseimic fault stress rate, J. Geophys. Res., 103, 24567–24572, https://doi.org/10.1029/98JB00594, 1998.

Wilcock, W. S. D.: Tidal triggering of microearthquakes on the Juan de Fuca Ridge, Geophys. Res. Lett., 28, 3999–4002, https://doi.org/10.1029/2001GL013370, 2001.

Wyss, M.: Towards a physical understanding of the earthquake frequency distribution, J. R. Astron. Soc., 31, 341–359, 1973.

Xu, Y. J., Wu, X. P., Yan, C. H., Huang, Y., Wang, Y., and Li, T.: The features of tidal Coulomb failure stresses on various kinds of seismic fault, Chinese J. Geophys., 54, 756–763, 2011.

Yan, L., Ren, Y., Chen, C., Yao, J., Chen, W., Huang, X., and Wang, S.: Geographic epidemiology methods for analysis of disease outbreaks in an county after Wenchuan earthquake, Geo-Inf. Sci., 11, 349–354, 2009.

Yang, W. Z. and Ma, L.: Seismicity acceleration model and its application to several earthquake regions in China, Acta Seismol. Sin., 21, 32–41, 1999.

Zhang, J., Qi, Q. W., Yang, L. Z., Chen, R. H., and Wang, W. X.: A study on tidal force/stress triggering of strong earthquakes, Chinese J. Geophys., 50, 448–454, 2007.

Zhang, S. X., Lu, X. J., Wang, Y. R., Jia, L. F., Zhang, G. L., and Shan, L. J.: Characteristics of accelerating moment release before the earthquake in northern China, Earthquake, 34, 49–57, 2014.

Zhang, Y., Feng, W., Xu, L., Zhou, C., and Chen, Y.: Spatio-temporal rupture process of the 2008 great Wenchuan earthquake, Sci. China Ser. D, 52, 145–154, https://doi.org/10.3321/j.issn:1006-9267.2008.10.002, 2008.

Zhao, Y. Z. and Wu, Z. L.: Mapping the *b*-values along the Longmenshan fault zone before and after the 12 May 2008, Wenchuan, China, M_S 8.0 earthquake, Nat. Hazards Earth Syst. Sci., 8, 1375–1385, https://doi.org/10.5194/nhess-8-1375-2008, 2008.

Zhu, Q. and Wang, Y.: Research on the restoration and protection of post-disaster ecological environment in Wenchuan county, Western China Development Review, Sichuan University Press, 50–57, ISBN 978-7-5614-6652-0, 2013.